Oceanic germanium/silicon ratios: Evaluation of the potential overprint of temperature on weathering signals

Douglas E. Hammond
Department of Earth Sciences, University of Southern California, Los Angeles, California, USA

James McManus
College of Oceanic and Atmospheric Sciences, Oregon State University, Corvallis, Oregon, USA

William M. Berelson
Department of Earth Sciences, University of Southern California, Los Angeles, California, USA

Received 11 June 2003; revised 4 February 2004; accepted 23 March 2004; published 18 May 2004.

[1] Diatom remains indicate the oceanic Ge/Si ratio (μmol/mol) has varied temporally, ranging from Miocene values of 0.9 to Last Glacial Maximum (LGM) values of 0.55, with the present value of 0.69. These ratios lie between those for the primary sources for these elements: continental weathering (Ge/Si = 0.5) and hydrothermal fluids (Ge/Si = 11). Previous explanations for temporal variation have focused on variations in the relative strength of the primary inputs. Alternatively, the cause may be temporal variation in the relative strength of the two sinks for Ge, opal, and a nonopal sink found in margin sediments. The importance of the latter depends on the rate of opal rain to the seafloor in margin environments. As temperature decreases, opal dissolution rates in the water column decrease, permitting a larger fraction of the opal rain to reach the seafloor before dissolving. This increases the rate of Ge uptake into nonopal phases. A model calculation predicts that a decrease of 3.5°C in LGM ocean temperature should increase opal rain to the margin seafloor by a factor of 1.5; an increase of 3.5°C in Miocene temperature should decrease rain by a factor of 0.6. The predicted changes for Ge uptake in the nonopal sink can account for essentially all of the temporal Ge/Si variation recorded in diatoms. The absence of larger changes constrains silicate weathering rates relative to the present as 106 ± 16% during the LGM and 88 ± 12% during the mid-Miocene (15–20 Ma). However, additional uncertainty exists because some factors of potential importance remain unconstrained. *INDEX TERMS:* 0330 Atmospheric Composition and Structure: Geochemical cycles; 1050 Geochemistry: Marine geochemistry (4835, 4850); 1886 Hydrology: Weathering (1625); 4845 Oceanography: Biological and Chemical: Nutrients and nutrient cycling; 4267 Oceanography: General: Paleoceanography; *KEYWORDS:* germanium, silicon, weathering

Citation: Hammond, D. E., J. McManus, and W. M. Berelson (2004), Oceanic germanium/silicon ratios: Evaluation of the potential overprint of temperature on weathering signals, *Paleoceanography*, *19*, PA2016, doi:10.1029/2003PA000940.

1. Introduction

[2] Changes in ocean chemistry during the past provide clues for elucidating linkages between biogeochemical cycles and Earth's climate system. The objective of this article is to explore a possible linkage between climate and the marine cycle of silicon. The importance of this linkage lies in the role Si plays in regulating diatom growth, as Si is an essential element for these organisms and its availability in the photic zone is frequently limiting in many parts of the ocean. Diatoms have been recognized as one of the principal agents for carbon export from the photic zone, so changes in the Si cycle may alter ocean ecology and influence the carbon cycle and atmospheric CO2.

[3] Clues about changes in the Si cycle may be found in the Ge/Si ratio preserved in diatoms. Modern diatoms recovered from core tops appear to record the oceanic ratio with good fidelity [*Bareille et al.*, 1998], so the diatom record should be a good representation of seawater composition. Diatom Ge/Si has been shown to vary in phase with changes in Earth's climate [*Shemesh et al.*, 1989; *Bareille et al.*, 1998]. During the Last Glacial Maximum (LGM), the ratio (all given in ru = μmol/mol) was approximately 0.55 ± 0.03, about 20% lower than the Holocene value of 0.69 ± 0.03 [*Bareille et al.*, 1998]. During the time period from 15 to 20 Ma (the late early Miocene and mid-Miocene, referred to subsequently as mid-Miocene), the ratio was larger, about 0.90, with distinct drops during cold episodes [*Shemesh et al.*, 1989]. During the late Pliocene/early Pleistocene cooling, the ratio dropped from 0.7–1.2 to 0.4–0.8 [*Lin and Chen*, 2002]. Although the correlation indicating higher Ge/Si ratios during warmer climates seems quite clear, the mechanism relating these two variables has been enigmatic.

[4] *Froelich et al.* [1992] reviewed the relationship between water column cycles of Ge and Si. Both elements are effectively removed from surface waters, primarily by diatoms, and released to deep waters by dissolution of the sinking opal tests. The internal cycling of these two

0883-8305/04/2003PA000940$12.00

Table 1. Budgets for Si and Ge in the Ocean[a]

	Si, 10^{12} mol yr^{-1}	Ge, 10^{6} mol yr^{-1}	Ge/Si, ru
	Inputs		
Rivers	5.6 ± 0.6[b]	3.0 ± 0.4	0.54[c]
Eolian	0.5 ± 0.5[b]	0.3 ± 0.3	(0.54)
Submarine weathering	0.4 ± 0.3[b]	0.2 ± 0.2	(0.54)
Hydrothermal	0.55 ± 0.25[d]	6.0 ± 3.2	11 ± 3[e]
Total	7.1 ± 0.9	9.5 ± 3.2	1.34 ± 0.36
	Sinks		
High latitude opal	4.1[f]	2.8	0.69 ± 0.03[g]
Other deep sea opal	<0.2[f]	<0.1	(0.69 ± 0.03)
Estuary opal	<0.6[f]	<0.4	(0.69 ± 0.03)
Margin opal	2.4–2.5[f]	1.7–1.8	(0.69 ± 0.03)
Margin nonopal		4.7 ± 3.2[h]	
Total	6.5–7.4[f]	9.5[h]	1.34[h]

[a]Values in parentheses are assumed on the basis of the ratio carried by rivers from weathering of soils. The Ge budget is calculated from Si budget and Ge/Si ratios, with loss balancing input. Uncertainties are calculated by error propagation.
[b]From *Treguer et al.* [1995].
[c]From *Froelich et al.* [1992].
[d]From *Elderfield and Schulz* [1996].
[e]From *Mortlock et al.* [1993].
[f]From *DeMaster* [2002].
[g]From *Bareille et al.* [1998].
[h]To balance inputs.

elements within the oceans is rapid when compared to their rates of input and removal, so the water column distribution of inorganic Ge (germanic acid) is linearly related to the abundance of Si (silicic acid). The linearity of the relationship and the near-zero intercept are strong evidence that little fractionation of these elements occurs during water column uptake and dissolution. Ge is also found in methylated forms, but these appear to have a residence time of a million years (more than 100 times that of inorganic Ge), and are considered to be unreactive. There are two principal sources of Ge and Si, weathering and hydrothermal inputs. Weathering is characterized by low Ge/Si ratios, while hydrothermal inputs have high ratios, with the present oceanic ratio of 0.72 ru falling between these sources (Table 1). Most previous efforts to explain the temporal variations in oceanic Ge/Si assumed that the principal sink for both elements is burial in opal. Under this assumption, variation in the relative strengths of these sources was the mechanism assumed to cause variations seen in the opal record, and the lower values during glacial times were interpreted as evidence for a doubling of weathering rates. Other studies have also proposed that glacial periods may have higher weathering. For example, *Gibbs and Kump* [1994] noted that a model simulation for global climate suggested higher runoff during glacial times, and that the exposure of continental shelves may have created slightly more land area for weathering. However, they also pointed out that these arguments predict increased carbonate accumulation during glacial times, and noted that this response has not been observed. An opposite perspective is posed by the strong evidence that glacial times were more arid. The lower atmospheric methane concentrations imply fewer wetlands [*Chappellaz et al.*, 1990]. Similarly, the lower $^{13}C/^{12}C$ of the glacial ocean and analysis of LGM biomes point to a decline in the quantity of terrestrial vegetation, as summarized by *Crowley* [1995]. Consequently, attributing changes in oceanic Ge/Si only to variations in weathering seems paradoxical, as it requires that colder and more arid glacial climates substantially enhance weathering and delivery of riverine Si to the ocean.

[5] Recent observations have identified a second major sink for Ge, with estimates that approximately half of the Ge removal occurs in a nonopal phase that forms in iron-rich, reducing sediments of continental margins [*Hammond et al.*, 2000; *King et al.*, 2000; *McManus et al.*, 2003]. This discovery offers a solution to the paradox noted above, because a variation in the relative importance of the opal and the nonopal sinks provides an alternative mechanism for explaining the linkage between oceanic Ge/Si and climate. The linkage is explored in this article, using a simple model calculation to show that the observed Ge/Si variation is likely to be a natural consequence of ocean temperature changes. The hypothesis is as follows. During colder climates, the dissolution rate of sinking opal tests is reduced, causing a larger fraction of the opal rain to reach the seafloor. Although most of this opal dissolves and is recycled, an increase in opal rain to the seafloor in margin areas (or any other area that can sequester Ge in nonopal phases) should increase the rate of Ge removal from the ocean in nonopal phases. This removal leads to a reduction in the oceanic Ge/Si, because less Ge must be buried in the opal phase.

2. Model Formulation

2.1. Oceanic Budgets for Ge and Si

[6] The Ge/Si ratio in the ocean is regulated by the budgets for each element (Table 1). The Si cycle has been considered by *Treguer et al.* [1995] and *DeMaster* [2002]. Sources and sinks in the modern ocean appear to be nearly in balance, with opal burial as the only significant removal

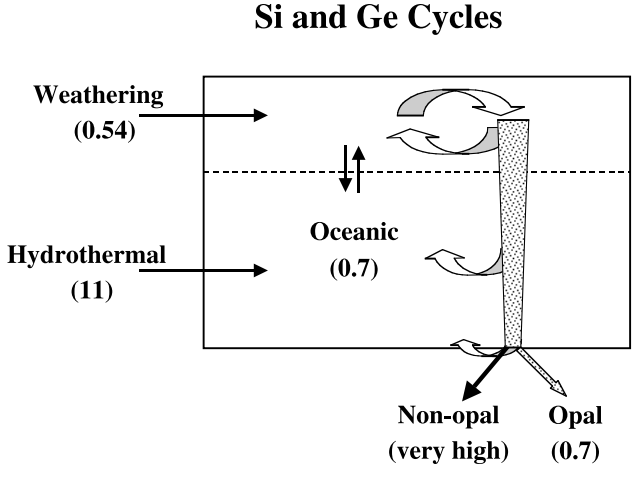

Figure 1. Box model illustrating the Si and Ge cycles. The Ge/Si ratios for sources and sinks are given in parentheses (μmol/mol). Arrows indicate fluxes. The weathering input is assumed to include dust dissolution. The nonopal sink is only significant for Ge.

mechanism. The residence time for Si is approximately 17 kyr, so the oceanic inventory of Si should be nearly in steady state through most of the Holocene. By contrast, two mechanisms remove significant Ge from the ocean, burial in opal and sequestration of Ge in a nonopal phase that forms in sediments with pore waters rich in ferrous iron. The magnitude of the latter sink is not precisely constrained by measurements at present, but is calculated by balancing the budget required by estimates for hydrothermal and weathering inputs. Although the nonopal phase(s) sequestering Ge has not yet been identified, this information is not necessary to define the budget. The Ge residence time is about half that for Si. During the Holocene, the ocean must have nearly attained a steady state, so the ratio for net input must equal the ratio removed.

2.2. Box Model Calculation

[7] *Hammond et al.* [2000] have presented a simple box model calculation to express the steady state balance for Ge and Si (Figure 1). It assumes there are two sources for each element. Two removal mechanisms are important, burial of both elements in opal and sequestration of Ge in a nonopal phase that forms in anoxic, iron-rich sediments that are most common in continental margins. The calculation assumes there is no fractionation of Ge and Si during opal formation because this effect appears to be small. Formulating this problem in a manner like that used for stable isotopes, the steady state expression relating the Ge/Si ratio (R) in the ocean to the input ratio and the diagenetic sequestration of Ge in a nonopal phase is:

$$R_{removal} = \alpha_d R_{ocean} = \alpha_d R_{opal} = R_{input}, \quad (1)$$

where

$$\alpha_d = \text{Ge/Si separation during diagenesis} = \left\{1 + S_{ge}\right\} \quad (2)$$

$$S_{ge} = \text{relative burial of Ge in the nonopal sink} = \sum A_i f_i J_{ni}, \quad (3)$$

with A_i, any fraction (i) of the seafloor that accumulates nonopal Ge; f_i, fraction of Ge sequestered from dissolving opal in region I; and J_{ni}, $\frac{\text{rain of opal that dissolves}}{\text{global average opal burial}}$ in region i.

[8] The summation includes the effect of all regions (i) that contribute to sequestration. The parameter J_{ni} reflects the rain of opal (mol cm^{-2} s^{-1}) that reaches the seafloor and dissolves in each local area where some Ge sequestration occurs. However, it has been normalized by the rate at which Si is removed from the entire ocean (opal burial rate in mol cm^{-2} s^{-1}), so the term appears to be dimensionless. The term S_{ge} represents the ratio (Ge buried in nonopal phases)/(Ge buried in opal). Mass balance constraints require that:

$$S_{ge} = \left(\frac{R_{input}}{R_{opal}} - 1\right). \quad (4)$$

Field observations led to an estimate that $S_{ge} = 1.0 \pm 1.0$, indicating that about half of the present Ge burial is in a nonopal phase [*Hammond et al.*, 2000]. Additional observations [*McManus et al.*, 2003] confirm this estimate as outlined in the next paragraph.

[9] At stations on the eastern margin of the Pacific, where upwelling is common and fractionation has been observed (Figure 2), f_i appears to be rather uniform, averaging 0.5 ± 0.1. The area of the seafloor involved is more difficult to estimate. Although fractionation has been observed in muddy shelf sediments, much of the shelf is characterized by coarse grained sediments that may be well irrigated by organisms and probably lack much Fe^{+2} in pore waters. Shallow water mobile mud belts and deltaic deposits may receive a high rain of opal and develop pore waters rich in ferrous iron, but these deposits appear to be fluidized and re-oxidized frequently [*Aller*, 1998]. If the re-oxidation destroys any ferrous-rich phase that may have sequestered Ge, these deposits may not account for significant Ge removal. Few areas in the deep sea receive sufficient carbon rain to become anoxic in the upper 2 cm, where most opal dissolves. Therefore little Ge should be sequestered in deep-water regions; pore water profiles [*Hammond et al.*, 2000; *King et al.*, 2000] are consistent with this interpretation. On this basis, the depth zone 200–2000 m (9% of the seafloor) seems a reasonable choice for A_i, although this area might have significant uncertainty. For comparison, *Morford and Emerson* [1999] estimated that 4% of the seafloor below 1000 m is characterized by sediments that are anoxic below 1 cm. Most sediments in depths 200–1000 m (4.4% of the seafloor) are also probably anoxic at rather shallow depths, leading to a minimum estimate of 8% for the area sequestering Ge. In the margin environments where Ge sequestration occurs, J_{ni} probably lies between 10 and 20. Entering these choices in equation (3) provides reasonable agreement with the value of $S_{ge} = 0.4–1.4$ required by equation (4) and the inputs in Table 1, and we assume the data in Table 1 adequately describe the present Ge and Si budgets. For reasons discussed in the following section, we assume that J_{ni} is the parameter that is most likely to be temperature-dependent. Because most opal reaching the margin seafloor dissolves, it should be proportional to the rain of opal to the seafloor in margin environments. The opal rain is simply a mechanism to shuttle Ge from the water column to the sediments. Once it is delivered to the seafloor, each Ge atom has a 50% chance of being buried in a nonopal phase.

2.3. Opal Dissolution Kinetics in the Water Column

[10] The rain of opal to the seafloor depends on its production and export from surface waters, its settling rate in sinking particles, and its dissolution rate. There is no information about how export and settling rate might vary with climate, but dissolution rate does depend on temperature. The simplest scenario is to hold the first two factors

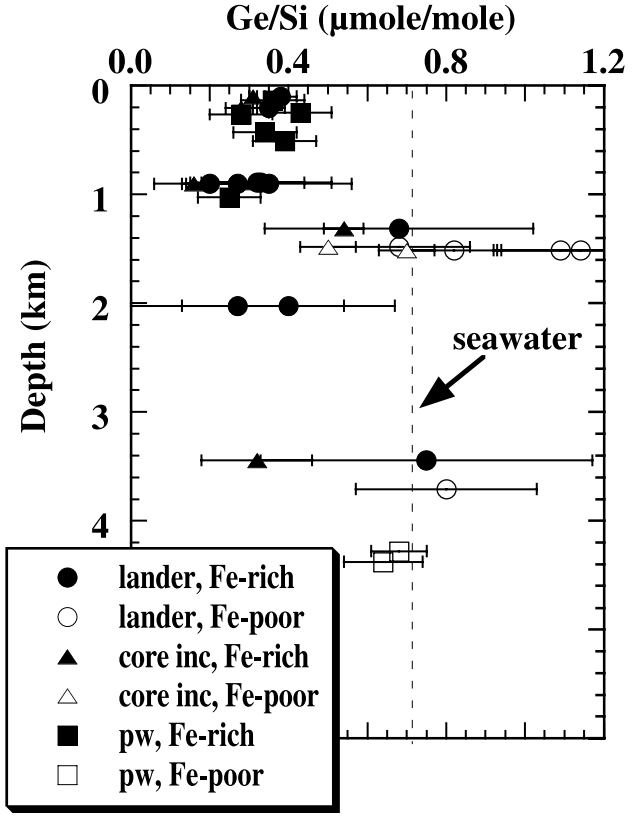

Figure 2. Ge/Si flux ratios released from opal dissolving in sediments. This is a compilation of observations for the California and Peru margins from *McManus et al.* [2003]. The two deepest sites are from the central equatorial Pacific. Techniques used to obtain these ratios include in situ flux chambers (lander), incubation of recovered cores, and calculation of fluxes from surficial pore water gradients (pw). Estimated uncertainty for the pw method is ±20%. Filled symbols are sites with significant pore water (Fe^{+2}) in the upper 2 cm. The average for these sites is 0.35 µmol/mol, half of the ratio for modern seawater (dotted line). This indicates that $f_i = 0.5 \pm 0.1$.

constant and assume that dissolution is first order with respect to opal availability and the rate constant follows an Arrhenius rate law:

$$R_z = \frac{dM_z}{dt} = M_z B \exp\left(\frac{-E_a}{R_{gas} T}\right), \quad (5)$$

where R_z is the dissolution rate of opal from sinking particles (mol s^{-1}), M_z is the opal in particles available to dissolve at depth z (mol), E_a is the activation energy, R_{gas} is the ideal gas constant, T is temperature (K) and B = constant characterizing dissolution (s^{-1}). Several values have been proposed for E_a. For example, *Van Cappellen and Qiu* [1997] found E_a = 48–75 kJ mol^{-1} for opal in Antarctic sediments. *Hurd and Birdwhistell* [1983] determined 75 kJ mol^{-1} for opal. They also noted that the enthalpy for dissolution is 20 kJ mol^{-1}, causing temperature to influence both solubility and dissolution kinetics with the functional form of equation (5), so E_a is used here to represent the sum of activation energy and enthalpy for dissolution. We did calculations for two values that bracket results obtained by most previous workers, using E_a = 65 and 95 kJ mol^{-1}. For these two values, the effect of temperature on reaction rate at 10°C is 9.8 and 14.3% $°C^{-1}$. Choosing the opal rain at 100 m as a reference horizon, the fraction of opal exported at 100 m that reaches the seafloor is related to the dissolution rate of sinking particles:

$$F_z = \frac{M_z}{M_{100}} = 1 - \frac{\int R_z dt}{M_{100}} = 1 - \int F_z B \exp\left(\frac{-E_a}{R_{gas} T}\right) dt, \quad (6)$$

where F_z is the fraction of the rain at z that has not dissolved in the water column and t is the time opal spends in the water column as it sinks from 100 m to the seafloor. The particle settling rate w = dz/dt can be used to transform time to depth, and the result is:

$$F_z = 1 - \int \left(\frac{B}{w}\right) F_z \exp\left(\frac{-E_a}{R_{gas} T}\right) dz, \quad (7)$$

integrated from 100 m to z.

[11] The ratio B/w was assumed to be independent of depth. It was estimated from values for F_z on the California

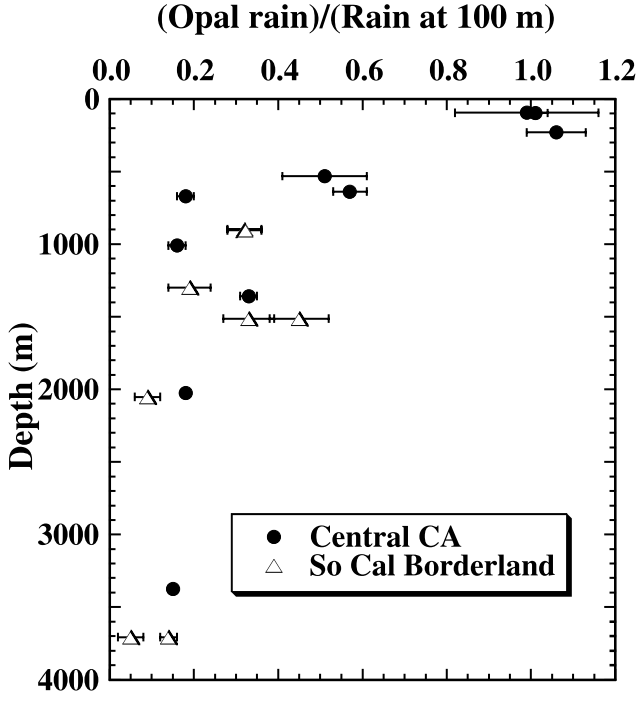

Figure 3. Opal dissolution on the California margin seafloor. Results have been determined using in situ benthic flux chambers, including measurements cited in the work of *Berelson et al.* [1996] and *Hammond et al.* [2000]. Data have been normalized to rain from the photic zone as noted in the text. Uncertainties from the normalizing factor for each region have not been considered in the error bars shown; these would make little difference for the central California results but could systematically shift all borderland points by up to 66% of each plotted value.

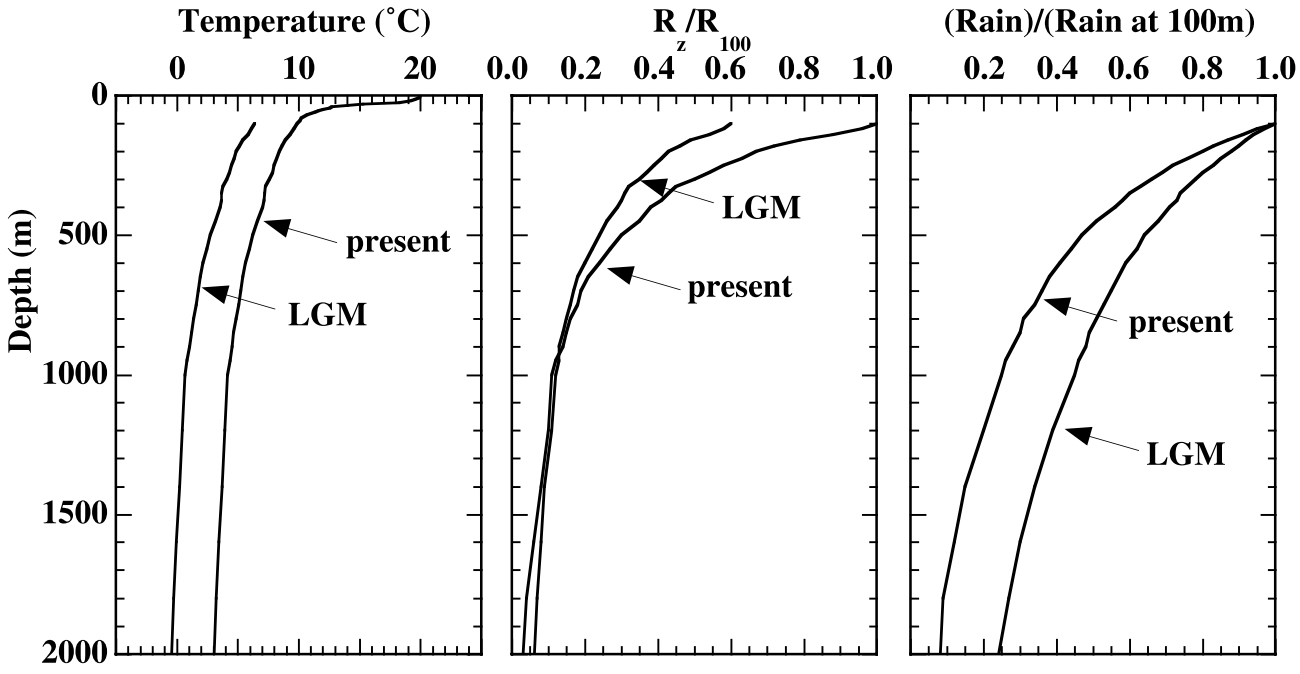

Figure 4. Sensitivity of dissolution rate to temperature change. The left panel is a typical temperature profile from the southern California borderland, a composite of data collected during July 2001 in San Nicolas Basin and further offshore. A scenario for the LGM is also shown, assuming a temperature decrease of 3.5°C throughout the water column (only data below 100 m are shown). The middle panel illustrates the rate at which opal should dissolve as it sinks through the water column as described in the text. Results are normalized by the rate at which it dissolves today at a depth of 100 m, where T is 10.0°C. Between 100 and 800 m, the large decrease for LGM reaction rate relative to present primarily reflects the temperature decrease. Below 800 m, the effect of LGM temperature decrease is nearly compensated by the increased opal rain reaching this depth. The right panel illustrates the fraction of opal rain at 100 m that survives dissolution in the water column and can reach sediments at each depth. An activation energy of 95 kJ mol^{-1} was used for this illustration. For this example, the present-day rate constant is 0.120 day^{-1} at the 100 m reference horizon if particles are assumed to sink 50 m day^{-1}.

Margin (Figure 3), based on the benthic flux measurements of *Berelson et al.* [1996], as follows. In this region, essentially all of the opal reaching the seafloor dissolves before it is permanently buried [*Berelson et al.*, 1987] so that the benthic flux of silicic acid from sediments characterizes the rain rate. For central California, the dissolution fluxes from sediments were normalized by measurements for a station at 100 m depth (averaging 7.5 ± 0.6 mmol m^{-2} day^{-1}). In the southern California borderland, analysis of silicic acid in surface waters at the SPOTS site (San Pedro Ocean time series) suggests the rain from surface waters is about 3 ± 2 mmol m^{-2} day^{-1} (W. M. Berelson, unpublished data, 2002), and this value was used to normalize measured fluxes. The large uncertainty for rain from surface waters of the borderland obscures any regional differences; we assumed the average flux at 1 km for both regions is about 25% of the rain from the photic zone. Equation (7) was integrated numerically from 100 m to 1 km, using the temperature profile in Figure 4a and iterating to find the value of B/w that resulted in F_{1km} = 0.25. The choice of 0.25 for this boundary condition is not very critical, as subsequent calculations only seek to evaluate the change in F_z due to changes in water column temperature. The calculated reaction rate (Figure 4b) decreases with depth, reflecting the decreases in both water temperature and available opal (Figure 4c) with depth.

[12] If water column temperatures decrease, the fraction of opal rain that dissolves while it is sinking decreases, and a greater fraction becomes available to dissolve in sediments (nearly all of the rain ultimately dissolves, even at the lower temperatures). During the LGM, estimates based on species assemblages for the California and Oregon Margins indicate that surface water temperatures were 1.5 to 3°C colder than at present [*Ortiz et al.*, 1997; *Pisias et al.*, 2001]. Even larger temperature changes have been estimated for the eastern equatorial Pacific and along the Peru coast, although smaller changes were estimated further offshore [*Feldberg and Mix*, 2002]. In the deep ocean, *Adkins et al.* [2002] determined that LGM temperatures from 2 to 4 km were 2.5 to 4.5°C colder than at present, indicating that the entire water column responds similarly to climate change. We assume LGM temperatures decreased 3.5 ± 1.0°C, based on the *Adkins et al.* [2002] reconstruction.

[13] The rain of opal to the seafloor (F_z) at all depths where Ge is sequestered in a nonopal phase (0.2–2 km) was computed using equation (7) and the LGM temperature

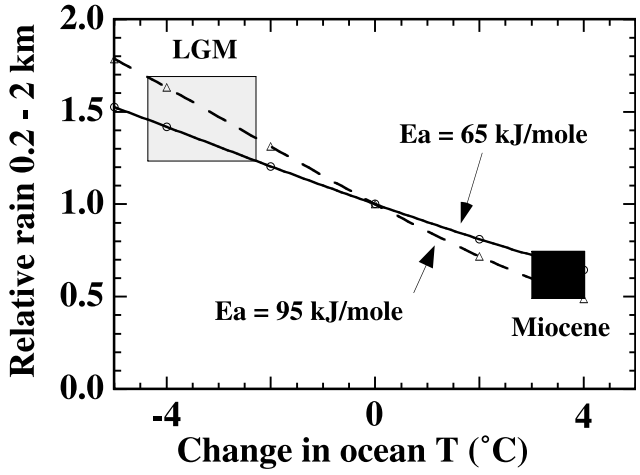

Figure 5. Sensitivity of opal rain to water column temperature. Simulations for the response of water column dissolution to temperature changes were used to predict the average rain of opal to the seafloor between 0.2 and 2 km. The result has been normalized by the average rain today. The solid and dashed lines show results for activation energies of 65 and 95 kJ mol^{-1}, respectively. The patterned boxes define the limits for range during past times, based temperature changes of −2.5 to −4.5°C in the LGM and 3–4°C in the Miocene. The boxes are defined by intersections of these temperature ranges with the dashed and dotted lines.

profile, assuming B/w is independent of climate. One scenario is shown in Figure 4. Next, the average for F_z through the 0.2–2 km depth range was calculated and compared to the present average for this depth range. For example, a 3.5°C decrease in ocean temperature should increase the average opal rain throughout the 0.2–2 km depth range by a factor of 1.36–1.55, depending on the activation energy used (Figure 5). The same computations were done for other temperatures. On the basis of the uncertainty of ±1°C for LGM temperature, the LGM conditions should lie within the field defined by the patterned box, with the average for opal rain to 0.2–2 km increasing by 1.26–1.71 times the present (Figure 5). A similar approach was used to estimate conditions for the Miocene, taking estimates of 3–4°C warming relative to today that are based on deep-water temperature changes [*Zachos et al.*, 2001]. The average opal rain to 0.2–2 km should have been 0.49–0.73 times the present (Figure 5). Note that these calculations assume that the export of opal at 100 m, the ratio B/w, the input of Ge, and the input of Si, do not vary with time; the only change is the fraction of opal export that survives dissolution in the water column and reaches the sediments in the 0.2–2 km zone, where Ge sequestration into nonopal phases should be most prevalent.

[14] The results in Figure 5 provide a measure of J_{ni} relative to the present, allowing the observed variation in Ge/Si to be compared to the predictions of equations (1)–(3) (Figure 6). Calculations assume that R_{input}, A_i and f_i do not vary with climate. The observed Ge/Si in opal for the LGM and Miocene are plotted with uncertainties in relative flux based on the results from Figure 5. As climate cools, the calculation predicts a decrease in the Ge/Si of opal. The decrease reflects the increase in the fraction of opal production that reaches the seafloor before dissolving, increasing the supply of Ge that can enter nonopal phases. On the basis of the best estimate for present R_{input} = 1.34 ru (Table 1), the calculated Ge/Si for LGM opal is similar to the observed ratio. An even better fit would have been obtained with a slightly larger value for present R_{input}. For the Miocene results, warming has the opposite effect on opal. The prediction based on R_{input} = 1.34 ru is within the estimated uncertainty, and a value for R_{input} = 1.70 would provide equally good agreement.

3. Discussion

[15] The model calculation illustrates the large effect that temperature is likely to have on the Ge/Si ratio of seawater and opal. This simple calculation accounts for most of the observed variation in the 3 climate regimes and is evidence

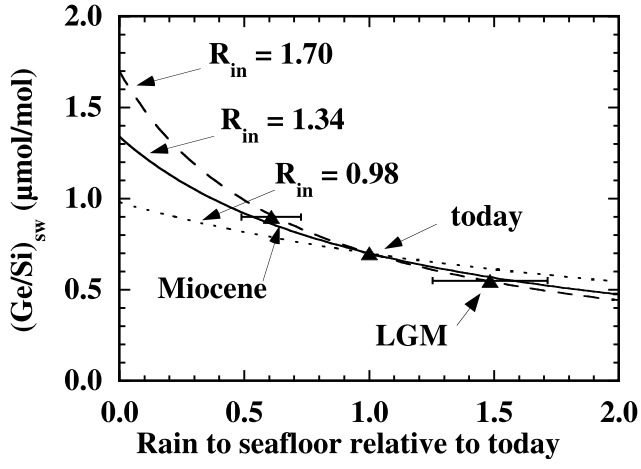

Figure 6. Ge/Si ratios related to opal rain. The Ge/Si of opal is plotted against opal rain relative to today. The results from Figure 5 were used to define the range for LGM and Miocene rain, and the mean of these is plotted against the Ge/Si ratios observed in diatoms of these ages (triangles). Equation (4) was used to predict the relation based on several choices for the ratio for Ge/Si inputs, assuming the ratio does not vary with time. The value of 1.34 is the best estimate for the present (Table 1), and the other lines illustrate relations expected at the limits defined by the estimated uncertainty for this value. All the observations could be fit well with any value for R_{in} of 1.3 to 2.0. The position of a data point relative to the line selected as the present value for R_{in} indicates whether weathering has differed in the past. A data point above this line would be evidence for lower weathering in the past, and a data point below this line would be evidence for greater weathering in the past. For example, if the present R_{in} is exactly 1.34, slightly less weathering occurred during the Miocene and slightly more during the LGM, relative to today.

that the ratio of Ge/Si inputs to the ocean have not varied greatly during the past 20 my. An important implication of this result is that if hydrothermal inputs have remained constant, the rate of silicate weathering during this time period has not varied by more than the uncertainties introduced by the factors in the equations. The following discussion focuses first on several critical assumptions made for the calculation and evaluates their implications. Second, although water column temperature change appears to be the dominant factor that changes Ge/Si, the absence of larger differences constrains how much variation in weathering has occurred during the time spanned by these observations. Finally, some of the broader implications for the LGM carbon cycle are reviewed.

3.1. No Ge/Si Fractionation During Opal Formation

[16] While recent work [*Ellwood and Maher*, 2003; *Rubin et al.*, 2002] suggests that in some settings there may be Ge/Si fractionation by diatoms in the water column, variations in this mechanism cannot be invoked as a primary cause of the difference between the Holocene and LGM. Two arguments support this logic. First, opal burial occurs primarily in high latitudes (about 50%) as well as in margins and marginal seas [*DeMaster*, 2002]. Both Ge and Si are largely removed from surface water in these regions, so the Ge/Si exported in opal must nearly equal the ratio in which they are supplied by upwelling from the deep sea. Consequently, core top ratios of modern sediments in high latitudes are very similar to seawater ratios [*Bareille et al.*, 1998]. Second, as pointed out by *Bareille et al.* [1998], if opal is the only sink for both elements, the burial ratio for the ocean must become close to the supply ratio within about one residence time (about 8 kyr for Ge). Even if fractionation during the LGM differed from today, the seawater Ge/Si would evolve to reflect this ratio. They also point out a corollary to this point. If fractionation occurred, the extent would depend on the fraction of Si utilized; the high latitude record shows that 6 Southern Ocean sites spanning 20° of latitude have comparable changes in the Ge/Si of opal during the present and past. It seems unlikely all these sites would have experienced similar partial Si drawdowns. Consequently, the model calculations ignore fractionation.

3.2. Role of Silicic Acid Profiles in Regulating Dissolution

[17] The calculation has ignored any effect of the silicic acid distribution in the water column, because the degree of saturation in the upper 2 km is generally less than 10%. It is possible that the profile of Si in the ocean has been different in the past due to differences in water column dissolution or due to changes in ocean circulation. However, these factors should also have only a modest effect on the degree of opal saturation or its dissolution rate.

3.3. Area of the Seafloor That Fractionates

[18] As noted above, shelf sediments may not be an important area for sequestering Ge. Consequently, changes in sea level may not affect the Ge budget very much. If shelf sediment area was a dominant factor regulating Ge removal from the ocean, and inputs of Ge and Si did not vary with time, the lowest Ge/Si ratios would be observed when sea level was highest. The opposite correlation is observed. What is more difficult to evaluate is the potential change in area of reducing sediments that may sequester Ge. Evidence for the eastern Pacific suggests that intermediate water was more oxic during the LGM than during the Holocene [*Ganeshram et al.*, 1995; *Kennett and Ingram*, 1995; *Dean et al.*, 1997], but other areas of the ocean may have been less oxic, such as the Atlantic sector of the Southern Ocean [*McManus et al.*, 1998]. The broad depth range over which present sequestration occurs (Figure 2) indicates that extremely low water column oxygen is not a requirement, and perhaps the area receiving a high rain of carbon to the seafloor is a more critical variable than the intensity of the oxygen minimum. Analyses of vanadium in foram shells provide a measure of the extent of reducing sediments, and the record for the last 35 kyr shows no detectable change [*Hastings et al.*, 1996]. However, the 100 kyr residence time of vanadium limits the sensitivity of this approach. Lacking data that demonstrate the contrary, we assume that the total area sequestering Ge did not change significantly from today, although its location may have varied. This point has been discussed in more detail elsewhere [*Hammond et al.*, 2000].

3.4. Constancy of B/w

[19] *Hutchins and Bruland* [1998] have shown that diatoms grown in iron-replete systems have lower Si/N uptake and consequently have less opal per test. In this case, mean diatom mass would decrease, and the fractional dissolution per unit time might increase. If LGM iron inputs to the margin were greater than at present, less silicified diatoms may have grown, increasing their specific dissolution rate and the constant B in equation (7). This idea is difficult to test because little opal is preserved in margin sediments to examine. However, margin areas generally have higher iron than open ocean areas, so the contrast between LGM and present conditions may not have been extreme. If diatom tests were less silicified, less opal would reach the seafloor, and less Ge sequestration would occur. We assume that changes in iron did not influence the specific reactivity of the opal that sinks in margin environments, because there is no evidence that reactivity was different than the present, and no other obvious mechanism has been identified that would act to compensate for such a change and reduce the oceanic Ge/Si ratio. A lower degree of silicification might also reduce w, the effective sinking velocity of opal. Most opal is probably transported in fecal pellets, and less silicification of diatoms could reduce the effective density of pellets. Particle settling rate may also be reduced due to an increase in water column viscosity as temperature decreases (2.5% $^{\circ}C^{-1}$). Countering such an effect is our inference that lower temperatures reduce opal dissolution, acting to keep the opal ballast in fecal pellets higher during the LGM than at present. Alternatively, the reason that large fecal pellets reach the seafloor may be that they settle so fast that they elude capture and destruction by midwater organisms. In this case, it may be that the effective velocity of fecal pellets determines their fate, and this might be insensitive to climate. Some support for this interpretation is the apparent increase in particle settling velocity with depth,

possibly due to the selective loss of the more slowly sinking particles [*Berelson*, 2002]. The factors governing particle dynamics in the water column are undoubtedly complex and are important to our hypothesis, but remain poorly understood. We assume that the envelope attributed to uncertainties in temperature change is sufficient to also include uncertainties introduced by possible changes in particle dynamics.

3.5. Weathering Rates Do Not Change at Other Times

[20] Results in Figure 6 show a trend similar to that predicted by the model calculation, and model results can be used to estimate the extent of variation in weathering/hydrothermal inputs in the past. If the best estimate for present $R_{input} = 1.34$ in Table 1 is correct and the model has perfectly estimated the effect of temperature on rain, then the observed Ge/Si ratio for the mid-Miocene lies slightly above the model calculation and the value for the LGM lies slightly below the calculation. If this difference is real, and reflects changes in R_{input} with time, it means that the ratio of hydrothermal/weathering inputs was slightly greater than today during the mid-Miocene and slightly less during the LGM. The observed ratios from the opal record were used to estimate the weathering inputs of Si in the past. These calculations assumed that the Ge/Si ratios for weathering and hydrothermal inputs do not vary, although *Froelich et al.* [1992] has suggested that the ratio in rivers may vary slightly if climate changes weathering intensity. *Murnane and Stallard* [1990] and *Filippelli et al.* [2000] have also noted effects of weathering intensity on ratios of Ge/Si in particular drainage basins, but we assumed that the global average for weathering intensity has not changed. Mass balances relate past weathering input of Si to the present, based on changes in hydrothermal inputs, Sge and the observed Ge/Si in opal:

$$\frac{W'_{si}}{W_{si}} = \left[\frac{H'_{si}}{H_{si}}\right]\left[\frac{\left(R_{input} - R_W\right)}{\left(R_H - R_{input}\right)}\right]_{today}\left[\frac{\left(R_H - R'_{opal}\left(1 + S'_{ge}\right)\right)}{\left(R'_{opal}\left(1 + S'_{ge}\right) - R_W\right)}\right] \quad (8)$$

where H_{si} indicates the hydrothermal flux of Si, R_i represents Ge/Si ratios for hydrothermal (H), weathering (W), and opal, and the primes denote past conditions. Results were calculated for several choices of present R_{input} and S_{ge}. The best estimates are that weathering was about 92 ± 12% of the present during the early/mid-Miocene, and about 106 ± 16% of the present during the LGM than at present. As noted earlier, these results indicate that any changes in weathering from the present were insufficient to produce changes that can be resolved by the Ge/Si proxy. These uncertainties are approximately one standard deviation, estimated by a root mean square approach because they are not symmetrically distributed about the value defined by our best estimate for model parameters. They were calculated by taking the deviations in relative weathering generated by independently varying R_{input} and S_{ge} by one standard deviation up and down, multiplying the differences of these 4 limits, and taking the fourth root of the product. An alternative approach would be to use the limits set by the parameter that introduces the greatest uncertainty in equation (8), R_{input}. This produces results that are 75 to 102% for the Miocene and 98 to 132% for the LGM.

[21] Independent estimates of weathering during the LGM are available. For example, a change in weathering should change opal accumulation. For the LGM, evidence for the Southern Ocean indicates that patterns of opal accumulation differed from the present, but the areally integrated rates were similar [*Chase et al.*, 2003]. This is consistent with the constraint above from Ge/Si, as any change of more than about 35% in the LGM global opal accumulation rate might be resolved in the sediment record. A second proxy is high precision analyses of Sr isotopes in forams. These do not show a change that is related to climate oscillations during the last 300 kyr and limit the amplitude of variation in Sr weathering input to <30% over the 100 kyr glacial/interglacial cycles [*Henderson et al.*, 1994]. Osmium isotopes in seawater provide a third proxy that should be even more sensitive to the response of weathering. Analyses of mid-Atlantic Ridge sediments by *Oxburgh* [1998] indicate that glacial values are consistent with a slightly reduced weathering during the LGM. While some uncertainty exists in defining the isotopic ratios of osmium in hydrothermal and weathering sources, the LGM results are consistent with glacial weathering that is about 15% lower than interglacial weathering. While it is possible that weathering of Si and Os could be de-coupled, there is no reason to expect this. Consequently, the evidence from all of these proxies suggests little difference in silicate weathering from the LGM to the present. The coherence of these proxies with results for Ge/Si is evidence that the model calculations for Ge are reasonable.

[22] The Miocene result deserves further discussion, as several aspects of the mid-Miocene (15–20 Ma) biogeochemical cycles could have been significantly different. First, *Engebretson et al.* [1992] have estimated global averages for past plate velocities. They found little difference during the past 20 my, although mid-Miocene rates may have been 5–10% less than at present. If their estimated plate motions were used as a proxy for hydrothermal input of Si, equation (8) indicates that a 5% reduction in Miocene hydrothermal inputs would lower the calculated rate of relative weathering by 5%. Second, mid-Miocene sea level was about 100 m higher than at present [*Haq et al.*, 1987]. This should reduce the continental area available for weathering by about 5%, relative to today (a hypsographic curve for present continents indicates a 100 m sea level rise should reduce land area by about 10% from the present, but half of this change would be compensated by the smaller area of ice sheets). However, the additional area covered by oceans will be of low relief, where little weathering may take place. Third, it is possible that the higher sea level and increased area for shallow water sedimentation provided some new regions for Ge sequestration. This would have kept the oceanic Ge/Si from rising closer to the input ratio. However, arguments presented earlier may rule out shelves as a major Ge sink. If they were a significant sink, Miocene weathering must have been even smaller than calculated. Measurements of

$^{187}Os/^{186}Os$ indicate the ratio has increased from 6 in the mid-Miocene to 8.6 at present [*Pegram et al.*, 1992]. However, it is uncertain whether this represents increased weathering at present, a change in the source rocks that are weathered, or both. Consequently, it is difficult to compare these results to those based on Ge/Si. The Ge/Si evidence that weathering rates during the Miocene were similar to today is interesting in light of the extensive middle to late Miocene opal deposits that rim the North Pacific. Apparently, these deposits only reflect changes in ocean circulation that caused a shift in opal deposition from the equatorial Atlantic and Caribbean [*Barron*, 1986]. Increased silicate weathering is not required for their formation. For example, the diatom-rich mid-Miocene deposits found in the Monterey formation of the California Margin have opal accumulation rates <2 mg cm^{-2} yr^{-1} during the 15–20 Ma time interval [*Isaacs*, 2001]. If the entire area of opal-rich deposits defined by *Ingle* [1981], about 8×10^6 km^2, was characterized by accumulation at this rate, it would only amount to <40% of the present Si input.

3.6. Potential Effects on the LGM Carbon Cycle

[23] The evidence that weathering during the LGM was similar to the present is interesting in light of suggestions that an increase in the oceanic Si inventory may stimulate diatom production and suppress coccolith production of $CaCO_3$ [*Archer et al.*, 2000; *Harrison*, 2000]. *Archer et al.* [2000] used a global circulation model that incorporated biogeochemical factors and found that the Si inventory must increase by a factor of 2–2.5 to suppress carbonate production sufficiently that atmospheric pCO2 would drop to values observed during the LGM. This would require doubling Si input if Si inventory is linearly related to weathering. *Harrison* [2000] linked diatom primary productivity to Si input and estimated the increase required to suppress coccolith productivity by 40%. Depending on the response of flagellates to increased diatom production, he noted that Si input must rise by 10–50%. This change is probably a lower limit for what is required, because he chose a value for Si gross production that is on the high end of those suggested by *Treguer et al.* [1995] and he did not consider the effect that lower LGM temperature may have in increasing the efficiency of Si export (an effect that would reduce its role in gross productivity). Assuming Si recycling in the photic zone is reduced by 15% for a 2°C temperature decrease, the Si inventory in LGM deep water must rise by 25–80% to provide his diatom productivity scenarios. *Harrison* [2000] proposed that Si input rose because dust dissolution increased, pointing out that estimates of eolian dust flux deposited in the deep sea during the LGM are 2–10 times greater than at present and might more than compensate for any decrease in riverine Si flux as temperature decreased. If river input of Si during the LGM was equal to the present, a four-fold increase in dust dissolution (assumed to have the same Ge/Si as rivers) would increase the Si supply to the ocean by about 25%. Such an increase is on the upper end of what is permitted by the Ge/Si and Os budgetary constraints, but is on the very low end of what is needed to explain the glacial/interglacial pCO2 change. Consequently, some role for changes in the weathering inputs of Si cannot be ruled out as a factor in changing pCO2, but it does not appear to be a primary cause.

3.7. Tests of the Hypothesis

[24] A test for the hypothesis of increased opal rain to the seafloor during the LGM would be to look at records of opal accumulation in margin sediments. Unfortunately, good records are scarce and many may reflect local responses to upwelling and primary production, as well as lower water temperatures. For example, sediments under the California Current do not show coherent behavior, as LGM opal accumulation rates for southern and central California were higher than in the Holocene, but the pattern off Oregon is reversed [*Gardner et al.*, 1997]. In addition, we do not have a good understanding about how opal burial in the margins is related to opal rain. With records encompassing more regions, the net response may become more clear. A second interesting test would be to obtain a high-resolution record of Ge/Si to examine more carefully how the timing of the Ge/Si change is related to the timing of climate change. However, the relatively long time constant (8 kyr) of Ge, compared to the time constant for climate change, will make it difficult to extract information about the relative timing of changes in the Si cycle and those of climate.

4. Conclusions

[25] The Ge/Si record in diatoms correlates with ocean temperature changes. A likely cause for this correlation is the effect that temperature should have on the extent of opal dissolution as it sinks through the water column. Colder temperatures permit a larger fraction of the opal rain to reach the seafloor, causing an increase in the extent of diagenetic sequestration of Ge into a nonopal phase in reducing, iron-rich sediments. This should have lowered the Ge/Si of seawater during the LGM, as the diatom record indicates. If all other factors are held constant, model predictions based on estimated temperature changes agree well with observed Ge/Si changes. During the Miocene, warmer temperatures seem to have had the opposite effect, causing the Ge/Si in opal to increase. While the effect of temperature in regulating opal rain to the seafloor is the dominant factor modulating the Ge/Si ratio in the ocean, the changes observed help constrain past weathering inputs. During the LGM, weathering rates may have been slightly greater (6%) than the present, but any difference is less than the sensitivity of the Ge/Si proxy (about 20%). If an increase occurred, it may reflect greater dust dissolution in the more arid LGM world. However, even if Si input increased by up to 25% during the LGM, it is unclear to what extent this might increase the oceanic inventory of Si. The lower LGM temperature may have also increased the opal burial efficiency and compensated for this effect. During the Miocene, the Ge/Si ratio is consistent with a slight reduction (about 8%) in silicate weathering, although this change is less than the estimated uncertainty. The cause of any reduction is unidentified. It is somewhat surprising that an increase was not observed in response to warmer temperatures during the Miocene.

[26] The scenario proposed does not constrain all factors that may help regulate the Ge/Si preserved in diatoms. Additional variables may play a role, but cannot be adequately constrained at present. One critical assumption is whether the opal raining to the margin seafloor in the past had dissolution kinetics similar to modern opal. A second assumption is whether the areal extent of sediments that sequester Ge has changed through time. This is particularly important during the Miocene, when higher sea level increased shallow water depositional areas. The impact of this factor on the Ge budget is difficult to constrain. Finally, the mechanism proposed here may not be a unique solution to the linkage between Ge sequestration in margin sediments and climate. It is possible that other factors have increased the rain of opal to the seafloor in margin environments, increasing the importance of Ge sequestration into nonopal phases. One possible effect during the LGM could be a reduction in the Si/N uptake of Southern Ocean diatoms in response to increasing iron, permitting more Si to be exported to low latitudes in intermediate waters, augmenting low latitude diatom production at the expense of coccoliths [*Brzezinski et al.*, 2002]. If such a change also resulted in higher export of opal in the margins, but the opal produced was less robust and had a higher specific surface area, one effect might happen to exactly compensate the influence of the other on Ge sequestration. Although the model calculation we have presented here may not be a unique interpretation, it does predict the direction and magnitude of change in diatom Ge/Si that is observed as temperature changes.

[27] **Acknowledgments.** Thoughtful reviews by Dave DeMaster and Gabe Filippelli, as well as discussions with Bob Aller, Steve Emerson, Nikki Gruber, and Frank Kyte stimulated further thinking about these concepts. The hospitality of Gary Klinkhammer and COAS at OSU facilitated preparation of this manuscript. Financial support was provided by National Science Foundation grants OCE 9911608 to DEH, and OCE 9911550 and OCE 0241372 to JM.

References

Adkins, J. F., K. McIntyre, and D. P. Schrag (2002), The salinity, temperature and d18O of the glacial deep ocean, *Science*, *298*, 1769–1773.

Aller, R. C. (1998), Mobile deltaic and continental shelf muds as suboxic, fluidized bed reactors, *Mar. Chem.*, *61*, 143–155.

Archer, D., A. Winguth, D. Lea, and N. Mahowald (2000), What caused the glacial/interglacial atmospheric pCO2 cycles?, *Rev. Geophys.*, *38*, 159–189.

Bareille, G., M. Labracherie, R. A. Mortlock, E. Maier-Reimer, and P. N. Froelich (1998), A test of (Ge/Si)opal as a paleorecorder of (Ge/Si)seawater, *Geology*, *26*, 179–182.

Barron, J. (1986), Paleoceanographic and tectonic controls on deposition of the Monterey Formation and related siliceous rocks in California, *Palaeogeogr. Palaeoclimatol. Palaeoecol.*, *53*, 27–45.

Berelson, W. M. (2002), Particle settling rates increase with depth in the ocean, *Deep Sea Res. Part II*, *49*, 237–251.

Berelson, W. M., D. E. Hammond, and K. S. Johnson (1987), Benthic fluxes and the cycling of biogenic silica and carbon in two southern California borderland basins, *Geochim. Cosmochim. Acta*, *51*, 1345–1363.

Berelson, W. M., J. McManus, K. H. Coale, K. S. Johnson, T. Kilgore, D. Burdige, and C. Pilskaln (1996), Biogenic matter diagenesis on the sea floor: A comparison between two continental margin transects, *J. Mar. Res.*, *54*, 731–762.

Brzezinski, M., C. Pride, V. Franck, D. Sigman, J. Sarmiento, K. Matsumoto, N. Gruber, G. Rau, and K. Coale (2002), A switch from Si(OH)4 to NO3- depletion in the glacial Southern Ocean, *Geophys. Res. Lett.*, *29*(12), 1564, doi:10.1029/2001GL014349.

Chappellaz, J., J. M. Barnola, D. Raynaud, U. S. Korotkevich, and C. Lorius (1990), Ice-core record of atmospheric methane over the past 160,000 years, *Nature*, *345*, 127–131.

Chase, Z., R. F. Anderson, M. Q. Fleisher, and P. W. Kubik (2003), Accumulation of biogenic and lithogenic material in the Pacific sector of the Southern Ocean during the past 40,000 years, *Deep Sea Res. Part II*, *50*, 799–832.

Crowley, T. J. (1995), Ice age terrestrial carbon changes revisited, *Glob. Biogeochem. Cycles*, *9*, 377–389.

Dean, W. E., J. V. Gardner, and D. Z. Piper (1997), Inorganic geochemical indicators of glacial-interglacial changes in productivity and anoxia on the California continental margin, *Geochim. Cosmochim. Acta*, *61*, 4507–4518.

DeMaster, D. J. (2002), The accumulation and cycling of biogenic silica in the Southern Ocean: revisiting the marine silica budget, *Deep Sea Res.*, *49*, 3155–3167.

Elderfield, H., and A. Schultz (1996), Mid-ocean ridge hydrothermal fluxes and the chemical composition of the ocean, *Annu. Rev. Earth Planet. Sci.*, *24*, 191–224.

Ellwood, M. J., and W. A. Maher (2003), Germanium cycling in the waters across a frontal zone: The Chatham Rise, New Zealand, *Mar. Chem.*, *80*, 145–159.

Engebretson, D. C., K. P. Kelley, H. J. Cashman, and M. A. Richards (1992), 180 million years of subduction, *GSA Today*, *2*, 93–100.

Feldberg, M. J., and A. C. Mix (2002), Sea-surface temperature estimates in the southeast Pacific based on planktonic foraminiferal species: Modern calibration and the Last Glacial Maximum, *Mar. Micropaleontol.*, *44*, 1–29.

Filippelli, G. M., J. W. Carnahan, L. A. Derry, and A. Kurtz (2000), Terrestrial paleorecords of Ge/Si cycling derived from lake diatoms, *Chem. Geol.*, *168*, 9–26.

Froelich, P. N., V. Blanc, R. A. Mortlock, S. N. Chilrud, W. Dunstan, A. Udomkit, and T. H. Peng (1992), River fluxes of dissolved silica to the ocean were higher during glacials: Ge/Si in diatoms, rivers and oceans, *Paleoceanography*, *7*, 739–767.

Ganeshram, R. S., T. F. Pedersen, S. E. Calvert, and J. W. Murray (1995), Large changes in oceanic nutrient inventories from glacial to interglacial periods, *Nature*, *376*, 755–758.

Gardner, J. V., W. E. Dean, and P. Dartnell (1997), Biogenic sedimentation beneath the California Current system for the past 30 kyr and its paleoceanographic significance, *Paleoceanography*, *12*, 207–225.

Gibbs, M. T., and L. R. Kump (1994), Global chemical erosion during the Last Glacial Maximum and the present: Sensitivity to changes in lithology and hydrology, *Paleoceanography*, *9*, 529–544.

Hammond, D. E., J. McManus, W. M. Berelson, C. Meredith, G. P. Klinkhammer, and K. H. Coale (2000), Diagenetic fractionation of Ge and Si in reducing sediments: The missing Ge sink and a possible mechanism to cause glacial/interglacial variations in oceanic Ge/Si, *Geochim. Cosmochim. Acta*, *64*, 2453–2465.

Haq, B. U., J. Hardenbol, and P. R. Vail (1987), Chronology of fluctuating sea levels since the Triassic, *Science*, *235*, 1156–1167.

Harrison, K. G. (2000), Role of increased marine silica input on paleo-pCO2 levels, *Paleoceanography*, *15*, 292–298.

Hastings, D. W., S. R. Emerson, and A. C. Mix (1996), Vanadium in forminiferal calcite as a tracer for changes in the areal extent of reducing sediments, *Paleoceanography*, *11*, 665–678.

Henderson, G. M., D. J. Martgel, R. K. O'Nions, and N. J. Shackleton (1994), Evolution of seawater 87Sr/86Sr over the last 400 ka: The absence of glacial/interglacial cycles, *Earth Planet. Sci. Lett.*, *128*, 643–651.

Hurd, D. C., and S. Birdwhistell (1983), On producing a more general model for biogenic silica dissolution, *Am. J. Sci.*, *283*, 1–28.

Hutchins, D. A., and K. W. Bruland (1998), Iron-limited diatom growth and Si:N uptake ratios in a coastal upwelling regime, *Nature*, *393*, 561–564.

Ingle, J. C., Jr. (1981), Origin of Neogene diatomites around the North Pacific rim, in *The Monterey Formation and Related Siliceous Rocks of California*, *Pacific Section SEPM Ser.*, vol. 15, edited by R. E. Garrison and R. G. Douglas, pp. 159–179, Pacific Section of the Soc. of Econ. Paleontol. and Mineral., Los Angeles.

Isaacs, C. M. (2001), Depositional framework of the Monterey Formation, California, in *The Monterey Formation: From Rocks to Molecules*, edited by C. M. Isaacs and J. Rullkotter, pp. 1–30, Columbia Univ. Press, New York.

Kennett, J., and B. Ingram (1995), A 20,000 year record of ocean circulation and climate change from the Santa Barbara basin, *Nature*, *377*, 510–514.

King, S. L., P. N. Froelich, and R. A. Jahnke (2000), Early diagenesis of germanium in sediments of the Antarctic South Atlantic: In search of the missing Ge-sink, *Geochim. Cosmochim. Acta*, *64*, 1375–1390.

Lin, H.-L., and C.-J. Chen (2002), A late Pliocene diatom Ge/Si record from the southeast Atlantic, *Mar. Geol.*, *180*, 151–161.

McManus, J., W. M. Berelson, G. P. Klinkhammer, K. S. Johnson, K. H. Coale, D. C. McCorkle, D. J. Burdige, D. E. Hammond, H. Brumsack, and A. Rushdi (1998), Geochemistry of barium in marine sediments: Implications for its use as a paleoceanographic proxy, *Geochim. Cosmochim. Acta*, *62*, 3453–3473.

McManus, J., D. E. Hammond, K. Cummins, G. P. Klinkhammer, and W. M. Berelson (2003), Diagenetic Ge-Si fractionation in continental margin environments: Further evidence for a non-opal Ge sink, *Geochim. Cosmochim. Acta*, *67*, 4545–4558.

Morford, J. L., and S. Emerson (1999), The geochemistry of redox sensitive trace metals in sediments, *Geochim. Cosmochim. Acta*, *63*, 1735–1750.

Mortlock, R. A., P. N. Froelich, R. A. Feely, G. J. Massoth, D. A. Butterfield, and J. E. Lupton (1993), Silica and germanium in Pacific Ocean hydrothermal vents and plumes, *Earth Planet. Sci. Lett.*, *119*, 365–378.

Murnane, R. J., and R. F. Stallard (1990), Germanium and silicon in rivers of the Orinoco drainage basin, *Nature*, *344*, 749–752.

Ortiz, J., A. Mix, S. Hostetler, and M. Kashgarian (1997), The California Current of the Last Glacial Maximum: Reconstruction at 42°N based on multiple proxies, *Paleoceanography*, *12*, 191–205.

Oxburgh, R. (1998), Variations in the osmium isotope composition of sea water over the past 200,000 years, *Earth Planet. Sci. Lett.*, *159*, 183–191.

Pegram, W. J., S. Krishnaswami, G. E. Ravizza, and K. K. Turekian (1992), The record of sea water 187Os/186Os variation through the Cenozoic, *Earth Planet. Sci. Lett.*, *113*, 569–576.

Pisias, N. G., A. C. Mix, and L. Heusser (2001), Millennial scale climate variability of the northeast Pacific Ocean and northwest North America based on radiolaria and pollen, *Quat. Sci. Rev.*, *20*, 1561–1576.

Rubin, S. I., J. W. Partin, and P. N. Froelich (2002), Biological fractionation of Ge/Si by Antarctic diatoms—JGOFS/AESOP trap results, *Eos Trans. AGU*, *83*(47), Fall Meet. Suppl., Abstract PP51A-0290.

Shemesh, A., R. A. Mortlock, and P. N. Froelich (1989), Late Cenozoic Ge/Si record of marine biogenic opal: Implications for variations of riverine fluxes to the ocean, *Paleoceanography*, *4*, 221–234.

Treguer, P., D. M. Nelson, A. J. Van Bennekom, D. J. DeMaster, A. Leynaert, and B. Queguiner (1995), The silica balance in the world ocean: A re-estimate, *Science*, *268*, 375–379.

Van Cappellen, P., and L. Qiu (1997), Biogenic silica dissolution in sediments of the Southern Ocean. II. Kinetics, *Deep Sea Res. Part II*, *44*, 1129–1149.

Zachos, J., et al. (2001), Trends, rhythms, and aberrations in global climate 65 Ma to present, *Science*, *292*, 686–693.

W. M. Berelson and D. E. Hammond, Department of Earth Sciences, University of Southern California, Los Angeles, CA 90089-0740, USA. (dhammond@usc.edu)

J. McManus, College of Oceanic and Atmospheric Sciences, 104 Ocean Admin Bldg., Oregon State University, Corvallis, OR 97331-5503, USA.